Astron. & Astrophys. 30, 423–430 (1974)

The Evolution of a Massive Protostar

I. Appenzeller and W. Tscharnuter
Universitäts-Sternwarte Göttingen

Received October 23, 1973

Summary. The hydrodynamic evolution of a massive protostar has been calculated starting from a homogeneous gas and dust cloud of $60\,M_\odot$ and an initial density of $10^{-19}\,\mathrm{g\,cm^{-3}}$. Initially the collapsing gas cloud evolved similar to protostar models of lower mass. About 3.6×10^5 years after the beginning of the collapse a small hydrostatic core was formed. About 2×10^4 years later hydrogen burning started in the center of the hydrostatic core. After another 2.5×10^4 years the collapse of the envelope was stopped and reversed by the heat flow from the interior and the entire envelope was blown off, leaving behind an almost normal main-sequence star of about $17\,M_\odot$. During most of the core's evolution the central region of the protostar would have looked like a cool but luminous infrared point source to an outside observer.

Key words: star formation – stellar evolution – infrared sources

I. Introduction

During the past several years hydrodynamic model calculations for the dynamical collapse of protostars have been carried out by various authors. (For a review of the literature see e.g. Hayashi, 1966; Larson, 1972b, 1973; Appenzeller, 1972). Although all these calculations were made using rather crude simplifying assumptions, their basic results were found to be in surprisingly good agreement with the observed properties of very young stellar objects and certain infrared point sources which are interpreted as protostars. However, all detailed dynamical computations published so far describe the evolution of low or intermediate mass protostars ($0.05 \leqq M/M_\odot \leqq 20$). Larson and Starrfield (1971) pointed out that (at least for the particular set of initial and boundary conditions used by these authors) massive protostars should evolve in a qualitatively different way, since in such objects nuclear reactions may start in the central regions while the outer layers are still in the stage of dynamical collapse. In order to investigate the fate of such a massive protostar in more detail, we computed in the present investigation the dynamical evolution of a $60\,M_\odot$ protostar. This mass was chosen, since it corresponds to largest stellar mass that has been determined directly from binary star observation (Sahade, 1962). Throughout the calculations we used the same rather crude simplifying assumptions which have been used in the earlier investigations of this kind. In particular we assumed the protostar to be always spherically symmetric, nonrotating, and non-magnetic.

II. Numerical Methods and Basic Assumptions

The evolution of the $60\,M_\odot$ protostar was calculated using a hydrodynamic stellar evolution computer program which has been described in an earlier paper (Appenzeller, 1970). However, in order to adapt the program to the special requirements of the protostars we modified the following details:

Energy Transport Equation

The radiative energy transport was always calculated according to the diffusion approximation

$$L_r = -\frac{64\pi^2 acr^4 T^3}{3\varkappa}\frac{\partial T}{\partial M_r} \tag{1}$$

[where, as in all following equations we use the same notation as used by Appenzeller (1970)]. This approximation is highly incorrect in the outer optically thin layers of the protostar. But, since these layers are in a state of almost free fall during most of the evolution, the approximation probably does not seriously affect the dynamical evolution. [A more detailed discussion of the error introduced by the above approximation has been given by Larson (1969, 1972a)]. In the later stages of the evolution of our $60\,M_\odot$ protostar a convective zone developed in the interior of the growing hydrostatic core. In these layers we simply replaced the radiative transport equation by the relation

$$\left(\frac{\partial \ln T}{\partial M_r}\right)\Big/\left(\frac{\partial \ln P}{\partial M_r}\right) = \nabla_{\mathrm{ad}} \tag{2}$$

(where ∇_{ad} is the adiabatic gradient). This relation assumes that convective energy transport is always so effective that the temperature gradient becomes adiabatic. Numerical estimates using the standard mixing length theory showed that Eq. (2) is certainly a good approximation for the late stages of the protostar's evolution but probably somewhat less accurate during the evolutionary phases just after the formation of the convective zone. In order to determine an upper limit for the error which was possibly introduced by Eq. (2) we also calculated the evolution neglecting all convective energy transport prior to the ignition of hydrogen. Although this resulted in a somewhat different structure of the core at the time of hydrogen ignition, we found no significant effects for the later stages of the protostar's evolution.

Equation of State

Our basic equations contain the density ϱ and the time derivative of the specific entropy $\partial S/\partial t$ which must be known as functions of the dependent variables P (total pressure) and T (temperature). For the present computations we used the relations

$$\varrho = P_{Gas}\frac{\mu}{\mathscr{R}T} \tag{3}$$

and

$$T\frac{\partial S}{\partial t} = \frac{\partial U}{\partial t} + P\frac{\partial V}{\partial t} = -\frac{P\cdot\delta}{\varrho}\left(\frac{\partial \ln P}{\partial t} - \nabla_{ad}^{-1}\frac{\partial \ln T}{\partial t}\right) \tag{4}$$

[where μ is the mean molecular weight and $\delta = -(\partial \ln\varrho/\partial \ln T)_P$]. In order to use Eqs. (3) and (4) μ, ∇_{ad}, and δ which in general again are functions of the temperature and the pressure, have to be known for all temperature and pressure values which occur during the model computations. Therefore, before starting our model computations we first calculated two-dimensional tables for μ, ∇_{ad}, and δ [as well as for $\alpha = (\partial \ln\varrho/\partial \ln P)_T$] using a tight grid of P and T values, which were then added to the computer program. During the model computations values for μ, ∇_{ad}, and δ were determined by interpolation in these tables.

In the optically thin outer layers of our protostar the dynamical effects of the radiation were always neglected since our crude treatment of the radiation flow in these regions did not allow us to take these effects into account. Thus, in the optically thin layers the gas pressure in Eq. (3) was always assumed to be equal to the total pressure or $P_{Gas} = P$. In the optically thick layers of the core the gas pressure was calculated according to

$$P_{Gas} = P - \frac{a}{3}T^4. \tag{5}$$

In calculating the tables for μ, ∇_{ad}, and δ the pressure and energy of the radiation field were also neglected. Therefore, in those layers where the radiation pressure was taken into account according to Eq. (5) the values of ∇_{ad} and δ had to be corrected for the effects of the radiation field. This correction was made in the main program before the values were inserted into the Eqs. (3) and (4).

For the computation of our tables of μ, ∇_{ad}, and δ we assumed that the gas consisted of H_2, H, H^+, He, He^+, He^{++}, the electrons and the heavier elements. The relative abundances of the different components as a function of temperature and (gas-) pressure as well as the corresponding values of the thermodynamic functions were calculated according to the standard methods described by Vardya (1960) and Mihalas (1966). However, since the hydrostatic cores of protostars initially reach relatively high densities at rather low temperature values, we found that electrostatic shileding effects on the ionization equilibrium (or "pressure ionization") are more important in such objects than in ordinary stars. Unfortunately, no generally accepted theory of this effect seems to be available (see e.g. Cox and Giuli, 1968). In the present computations the electrostatic interaction effects were taken into account using the corrected ionization potentials suggested by Ecker and Kroll (1965).

Opacity

For $T \geqq 5000\,°K$ the Rosseland mean absorption coefficients $\varkappa$ were taken from the tables of Cox and Stewart (1969). For $1300 < T < 5000\,°K$ we used the $\varkappa$-values calculated by Krügel (1971). Although calculated independently, Krügel's low temperature opacity values are generally similar to those used in other protostars computations (see e.g. Aumann and Bodenheimer, 1967; Narita *et al.*, 1970, Fig. 1). For temperatures below 1300 °K, where dust grains are the only important source of opacity, we used the dust absorption coefficients derived by Gaustad (1968). Due to the uncertainties of the composition of interstellar dust grains and of the broadening mechanisms of molecular lines at low temperatures, the opacity values for temperatures below 3000 °K are probably not more than rough approximations which may be wrong by as much as two powers of ten. Fortunately, test computations with artificially changed opacities indicate that even large changes of the opacity at these low temperatures have very little influence on the basic results of the model computations (Larson, 1972a).

Nuclear Reactions

Of the various nuclear reactions which may occur during the very early stages of stellar evolution we considered the conversion of hydrogen into helium only.

The energy generation due to the hydrogen burning was calculated using a subroutine taken from the hydrostatic stellar evolution code by Hofmeister *et al.* (1964). For the initial chemical composition of the protostar we assumed $X = 0.707$, $Y = 0.266$, $Z = 0.027$. The change of the chemical composition due to the hydrogen burning was neglected in the computations, since the time interval which we investigated was much shorter than the main-sequence life time of a massive star.

Difference Scheme

Except for a few minor changes (which were made in order to improve the internal numerical accuracy) we used the same difference equations as in our earlier hydrodynamic computations. In the early isothermal collapse phases (which correspond to most of the protostar's life time but only to about 2–3% of the total computing time) we used a fixed number of mass shells ($N = 156$). Later the changing structure of the core made it necessary to adjust the number and position of the mass shells frequently by an automatic procedure. In this phase the number of mass shells varied between 90 and 162 with an average number of about 150. The whole evolutionary sequence required about 3300 time steps of highly different length. In order to estimate the accuracy of our numerical integration procedure we repeated parts of the computations using different time steps and different numbers of mass shells. From these tests we estimate that the errors introduced by the finite differences are probably not larger than a few per cent. They are certainly smaller than the effects introduced by the uncertainties of the initial and boundary conditions described below.

III. Initial Values and Boundary Conditions

We started our computations with a stationary homogeneous spherical gas cloud of $60\,M_\odot$, with a density of $10^{-19}\,\mathrm{g\,cm^{-3}}$ (corresponding to a radius of $R = 6.5 \times 10^{17}$ cm), and a temperature of 150 °K. With these parameters the density of the cloud is slightly larger than the critical density for the gravitational instability. Qualitatively our initial conditions are therefore of the same type as those used by Larson (1969, 1972a). However, we used a considerably higher temperature since, following Pikel'ner (1970), we assume that massive stars originate from hotter interstellar matter (where the Jeans-length is larger) than the low mass stars. The properties of our initial gas cloud are in reasonable agreement (within one order of magnitude) with the corresponding data observed in the so called infrared nebulae and in certain interstellar molecular clouds.

Again following Larson (1969) we assumed that the outer boundary of the collapsing gas cloud remained

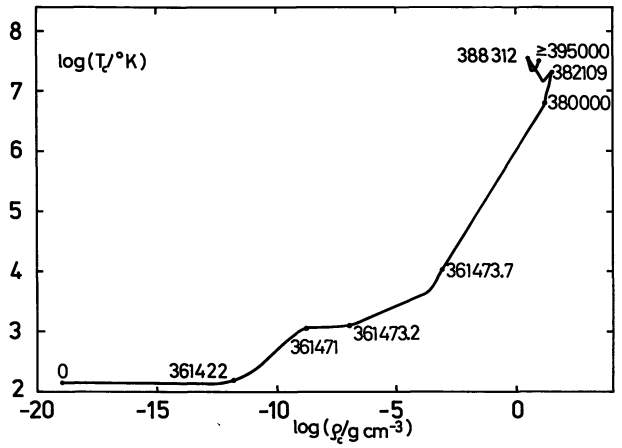

Fig. 1. The variation of the central temperature T_c and density ϱ_c during the evolution of a $60\,M_\odot$ protostar. The numbers indicate the protostar's age in years

fixed in space or

$$R = r(M_r = M) = \text{const} \qquad (6)$$

and that the temperature at this fixed boundary stayed constant at the initial value of 150 °K. As pointed out elsewhere (Appenzeller, 1972), test calculations with different boundary conditions show that at least during the early phases of the evolution of protostars the qualitative results are rather insensitive to the boundary conditions, but that the time scales of the evolution are changed. As pointed out in Section V of this paper, the time scale of the dynamical evolution may be rather important for the quantitative end-result of the evolution of massive protostars. Thus, it seems possible or even likely that the present results were influenced by the particular boundary condition which we have used. A reliable answer to this question can only be given by repeating the whole evolutionary sequence with different boundary conditions. Computations of this kind are in progress.

IV. Numerical Results

Our results for the early phases of the evolution of the $60\,M_\odot$ protostar are rather similar to those found by Larson (1969, 1972a) for protostars of lower mass. As in these calculations the collapsing gas cloud at first stayed optically thin and isothermal but became rapidly nonhomogeneous (c.f. Appenzeller, 1972, Fig. 2). As indicated in Fig. 1, about 3.6×10^5 years after the onset of the collapse the central region of the cloud became optically thick and the central temperature then started to increase. At an age of 361471 years a temporary hydrostatic core was formed. Initially this core contained about $0.03\,M_\odot$. Its initial Radius, central temperature and central density were $R = 4 \times 10^{13}$ cm, $T_c = 1290$ °K, $\varrho_c = 1.5 \times 10^{-9}\,\mathrm{g\,cm^{-3}}$. At the boundary

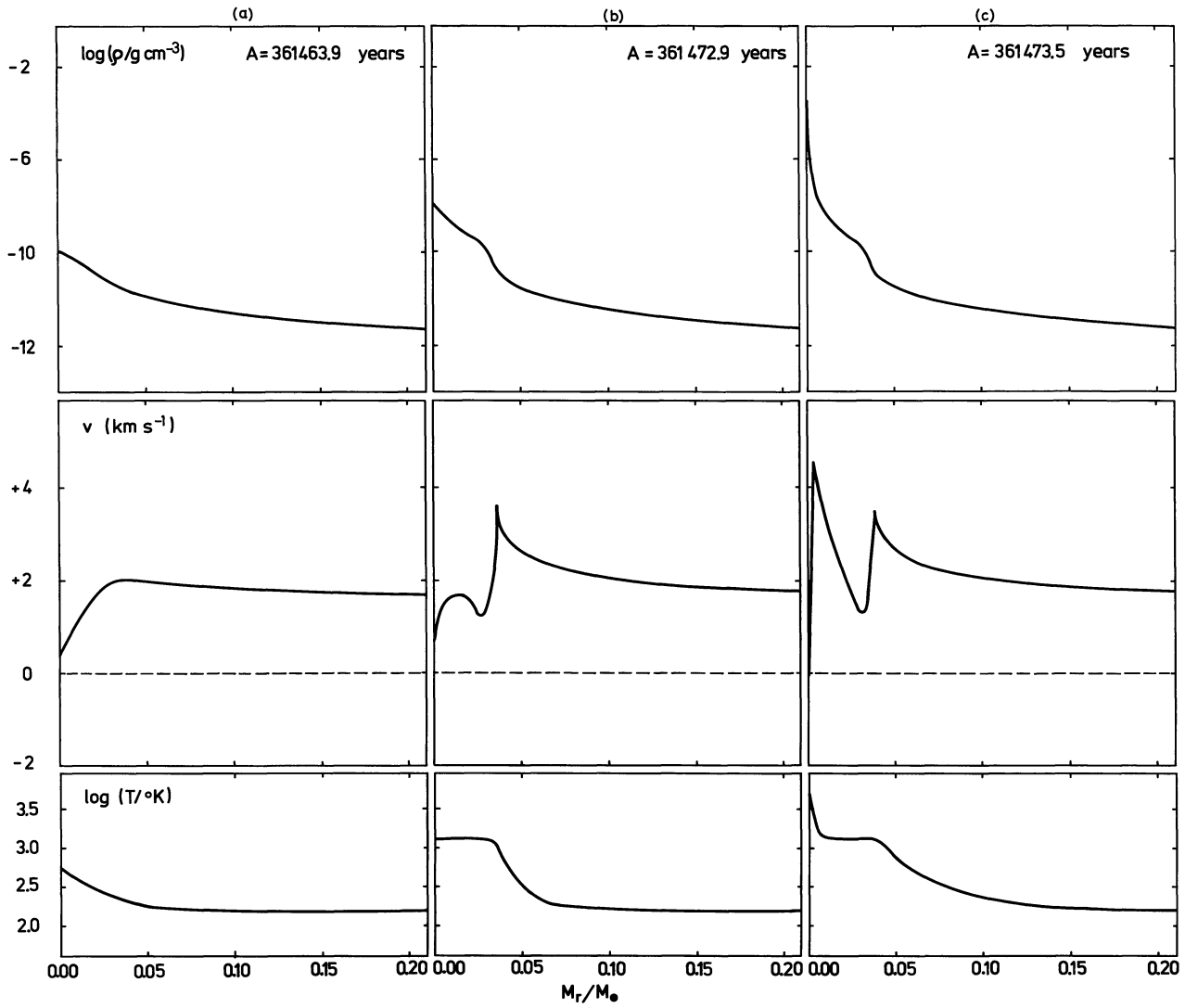

Fig. 2a–c. The density, infall velocity, and temperature distribution in the central region of the 60 $M_\odot$ protostar (a) shortly before the first (temporary) hydrostatic core starts to form, (b) two years after the formation of the temporary hydrostatic core (which in its central part just starts to collapse again), and (c) shortly after the formation of the second (final) hydrostatic core. The shock fronts (indicated by the sudden change of the velocity gradient) are artificially broadened using the artificial viscosity method

of the core a shock front was formed since the infall velocity was supersonic. Soon after the formation of the core the transparency of the matter in the interior of the core increased again (due to the evaporation of the dust grains) and the core became almost isothermal again. Because of this effect and because of the beginning of the dissociation of the hydrogen molecules the central temperature temporarily increased too slowly to maintain the hydrostatic equilibrium. Therefore, about two years after its formation the first hydrostatic core started to collapse again (Figs. 1 and 2). Only six months later the second (final) hydrostatic core was formed. Its initial parameters were $M_c = 0.004\, M_\odot$, $R = 1.7 \times 10^{12}$ cm, $T_c = 7050$ °K, $\varrho_c = 4.3 \times 10^{-4}$ g cm^{-3}. At the boundary of the second core again a shock front was formed where because of the smaller radius and larger gravitational acceleration the infall velocity soon became larger than at the outer shock front. During the following years the core had the rather complex structure shown in Fig. 3 where the two shock fronts now exist simultaneously. The position of the outer shock and the life time of this stage depend on the radiation flow from the hot inner shock to the matter just below the outer shock. Since the temperature of the matter between the shock fronts is about 10^3 °K, the opacity in these critical layers and the details of the evolution are rather uncertain in this phase. Fortunately, this evolutionary stage does not last very long and therefore it will probably not have much influence on the later evolution of the protostar. With the opacity values assumed in the present investigation the two shock fronts merged about 100 years after the formation of the hydrostatic cores. During the following $\sim 4 \times 10^4$ years the mass of the core increased slowly to about

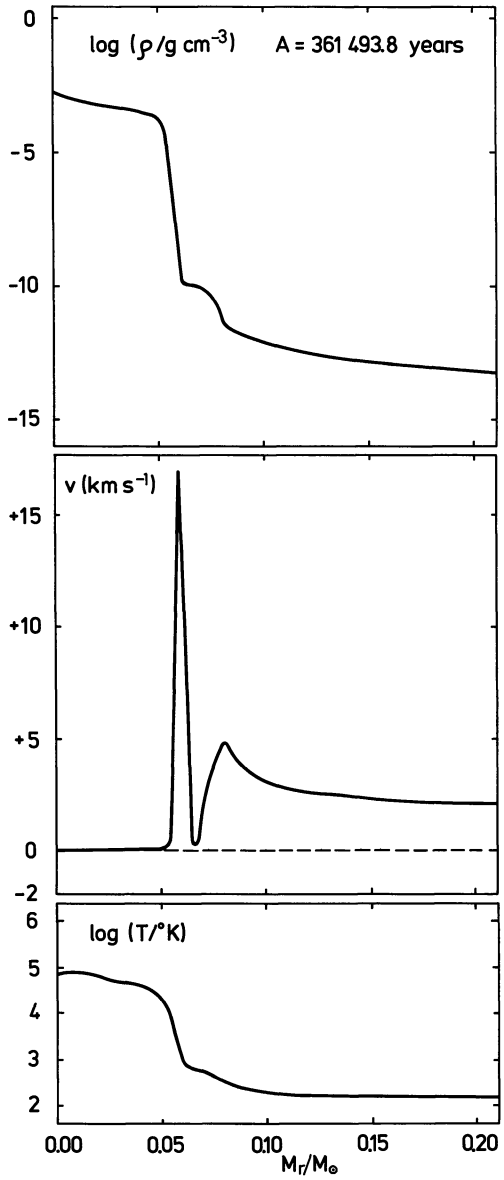

Fig. 3. The structure of the central region of the protostar 20 years after the formation of the final hydrostatic core

18 $M_\odot$ while (as illustrated by Fig. 4a, b) the basic structure of the protostar remained unchanged. However, as illustrated by Fig. 5, the interior of the core started its own evolution during this time interval. Initially the opacity in the core was increasing rapidly with the increasing density and temperature. As a result radiative energy transport soon became ineffective and a convective zone was formed. Due to the radiative losses shortly after the formation of the core at this stage a temperature inversion existed near the center of the core (c.f. Fig. 3). Because of the temperature inversion during the first 2×10^4 years the convection did not reach into the center.

At an age of about 3.8×10^5 years (or about 2×10^4 years after the formation of the core) in a small region near the center the temperature reached sufficiently high values to ignite the hydrogen. Although the hydrogen burning started in a rather small fraction of the core's mass, the high density and the small temperature gradient in the temperature inversion region resulted in a rather high total energy output during this initial burning phase. As a result of this sudden heat input the core expanded again while the central temperature decreased (c.f. Fig. 1). About 4×10^3 years after the ignition of hydrogen the central temperature reached a minimum and then slowly started to increase again. The central density still continued to decrease, however. Thus, at this stage the core of our protostar behaved like a massive main-sequence star of slowly growing mass. This is not surprising since initially the accretion of matter to the core continued essentially unaffected by the nuclear burning in the center. From this stage on we found it useful to compare the structure of the core with normal zero-age main-sequence models of equal mass which we calculated using the hydrostatic computer code of Hofmeister *et al.* (1964).

From this comparison the internal structure of the protostellar core was found to be qualitatively similar to the structure of the corresponding main-sequence models. However, the radius of the protostellar core (1 to 2×10^{12} cm) still turned out to be 3 to 5 times larger than the surface radius of the corresponding ZAMS models. A more detailed comparison showed that this was caused by a lower density of the outer layers of the protostellar core, while the central values of the density and temperature differed only little from the corresponding values of the main-sequence models. There are probably two reasons for this behaviour: First, the outermost layers of the core were still contracting slowly. In addition, the outer boundary of the core was not a normal stellar atmosphere but consisted of the relatively cool ($T \lesssim 10^4$ °K) but optically thick "intermediate layer" between the accretion shock and the surface of the core. In contrast to the optically thin envelope outside the accretion shock the dynamics of the matter in the "intermediate layer" was controlled by gas and radiation pressure. However, this matter was not yet at rest (as the matter in the core) but in a state of rapid compression. This "intermediate layer" and the outermost layers of the core were highly opaque to the radiation from the core. Therefore, most of the energy flow from the core was absorbed and converted into internal energy in these layers. However, in spite of the heating by the absorption of radiation and the pressure increase, the cool intermediate layer did not disappear; the matter which was heated at the lower boundary of the intermediate layer was replaced by the continuous inflow of new matter through the accretion shock.

After the ignition of hydrogen the energy flow from below increased. Therefore the layers below the shock started to expand and to push the shock outwards. The

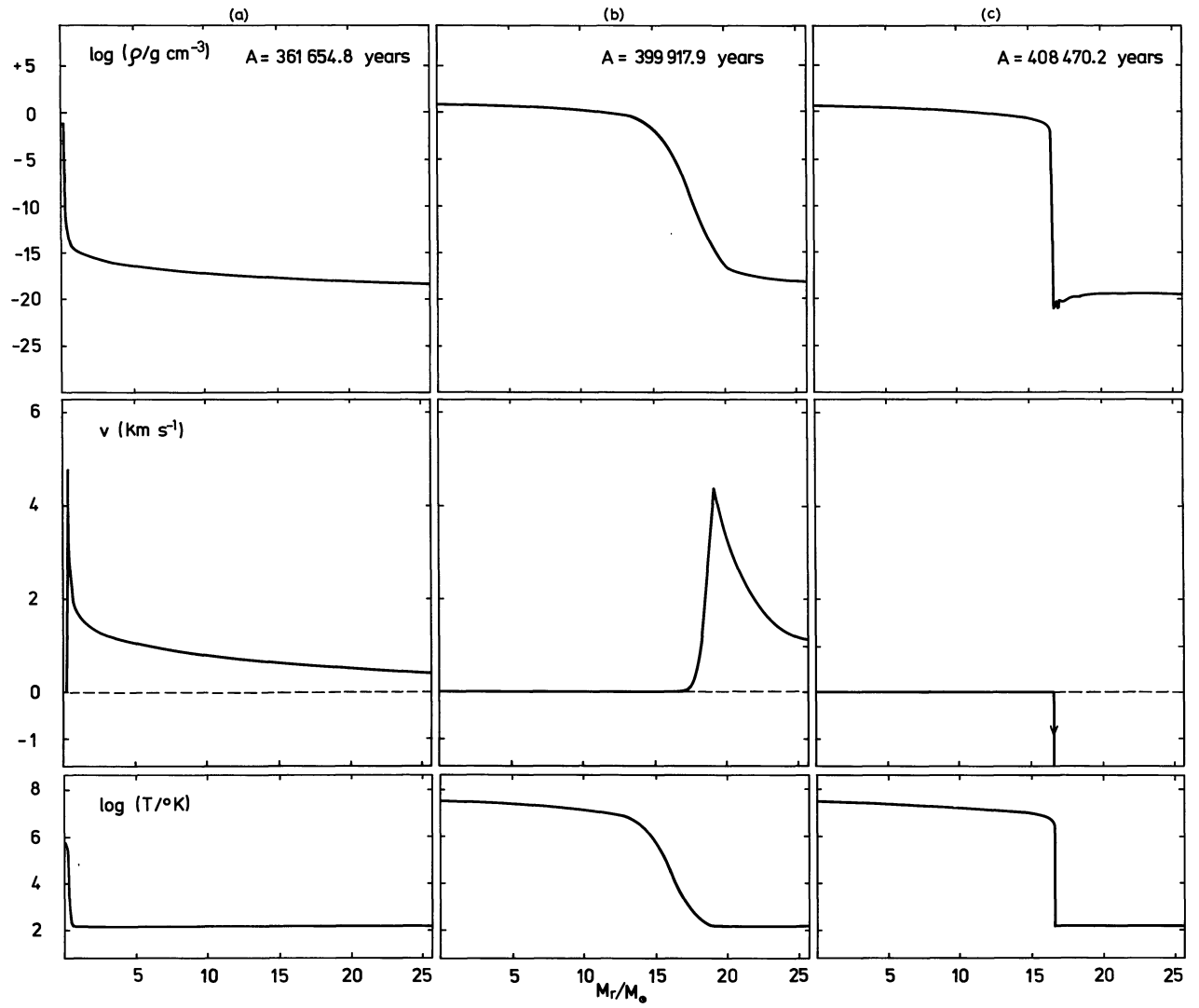

Fig. 4a–c. The structure of the protostar (a) after the merger of the two shock fronts, (b) towards the end of the accretion phase and (c) after the collapse of the envelope has been reversed. In part (c) of the figure the velocity in the envelope is directed outward (indicated by the negative sign of the infall velocity v) and far outside the diagram ($\gtrsim 10^2$ km s^{-1}), while the velocity in the core has become negligible

decreasing density, however, resulted in a stronger radiative energy flow from the interior which in turn resulted in a further expansion. Apparently through this feed-back mechanism the expansion of the outermost layers of the core accelerated slowly. Finally, about 4.5×10^4 years after the formation of the core ($\sim 2.5 \times 10^4$ years after the first ignition of the hydrogen) the energy inflow into the "intermediate layer" became so rapid that it could no longer compensate fast enough by a simple quasihydrostatic expansion. Therefore a pressure excess was built up and, as a result of this pressure excess, the inward motion of the matter just below the shock was stopped and reversed into a supersonic outward motion which eventually exceeded the escape velocity from the core. Due to this mass ejection and the rapid expansion of the matter just below the ejected layer the "intermediate layer" now became transparent to the radiation from the surface of the core. As a result the protostar's luminosity (as indicated in Fig. 6) increased by a factor of about 50 within a few years. Because of this rapid heat loss the outermost layers of the remaining hydrostatic core (which from now on contained a constant mass of 16.7 $M_\odot$) cooled down and started to contract again. This, in turn, resulted in a decrease of the luminosity and an increase of the effective temperature. As shown in Fig. 6, about 2×10^3 years after the flare-up both values rapidly approached the equilibrium values for a 17 $M_\odot$ zero-age main-sequence star. Except for the atmospheric layers, the internal structure of the hydrostatic core was now almost identical with that of our hydrostatic 16.0 $M_\odot$ main-sequence model.

The matter which was ejected from the surface of the core expanded rapidly and moved outward at velocities approaching several 10^2 km s^{-1}. As a result, a shock front now rapidly travelled through the whole envelope

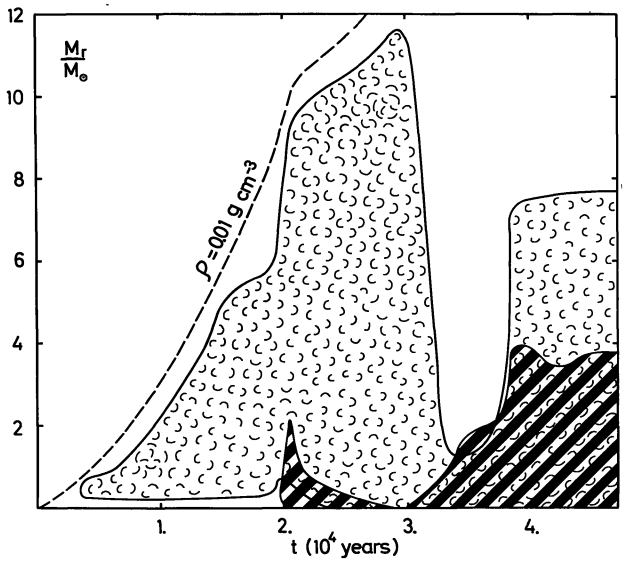

Fig. 5. The variation of the internal structure of the evolving hydrostatic core. The abscissa gives the time since the formation of the (final) hydrostatic core. ($t = 0$ corresponds to an age of the protostar of 361473 years.) "Cloudy" regions represent convection. Cross-hatched regions represent nuclear energy generation at a rate exceeding 10^3 erg g^{-1} s^{-1}. The approximate extent of the hydrostatic core is indicated by the line $\varrho = 0.01$ g cm^{-1}

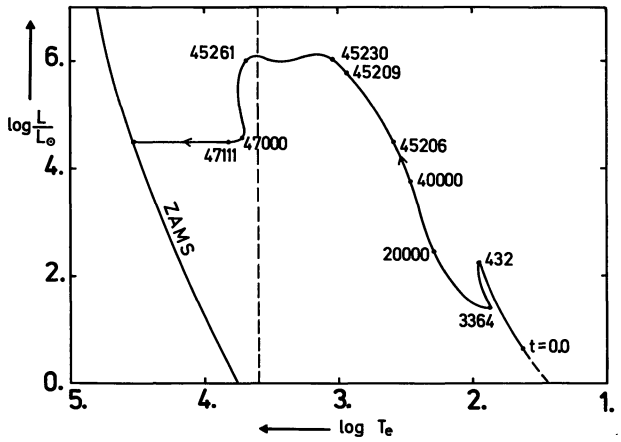

Fig. 6. Approximate evolutionary path of the optically thick central region of the 60 $M_\odot$ protostar in an infrared HR diagram. The numbers indicate the time t since the formation of the final hydrostatic core (c.f. Fig. 5). For comparison we also included the position of the zero-age main-sequence (ZAMS). The broken line gives the approximate lower limit of the effective temperature of hydrostatic configurations (Hayashi *et al.*, 1962)

of the protostar and practically all matter outside the core was accelerated to velocities above the local escape velocity. Thus, with a realistic boundary condition this matter would have been lost from the system. [Because of our too simple boundary condition Eq. (6) the escaping matter was reflected at the fixed outer boundary and, in fact, started to fall back on the core. This forced us to stop the computations shortly before the core reached its final equilibrium radius and effective temperature.] At this stage the radiation pressure of the visible and ultraviolet light photons on the dust in the envelope probably becomes most important. Since this effect was neglected, the density distribution and the velocity field in the expanding envelope derived in our computations is probably highly incorrect and will therefore not be discussed here.

V. Discussion

The results of our model computations confirm the prediction by Larson and Starrfield (1971) that in the case of massive protostars the infall of the envelope may be stopped by the energy flow from the evolving hydrostatic core long before all the matter of the original collapsing cloud has been accreted. According to the present calculations, as described in Section IV, the reversal of the collapse is triggered by changes in the layers just below the accretion shock. The properties of these layers depend on the accretion rate and therefore on the time cale of the dynamical collapse phase which is determined by the uncertain initial and boundary conditions. Thus, the fraction of the initial collapsing gas cloud which finally condenses into the resulting main-sequence star and other quantitative results of the present computations may depend critically on the initial and boundary conditions which we have assumed. Further work is needed to determine this dependence. However, the basic qualitative results described above should be typical for the evolution of nonrotating massive protostars and can probably only be changed by using rather unreasonable assumptions.

In Fig. 6 we plotted the approximate evolutionary path of the core of our protostar in an infrared HR diagram. Because of our crude treatment of the radiation flow in the optically thin layers, only the luminosity L could be taken directly from our calculations. The corresponding values of the effective temperature T_e were estimated from the relation

$$T_e = \left(\frac{1}{4\pi\sigma} \frac{L}{r_e^2} \right)^{\frac{1}{4}} \tag{7}$$

where r_e denotes the radius at which the optical depth $\tau = \frac{2}{3}$ is reached. In calculating τ the dust absorption in the outer – for infrared radiation transparent – part of the envelope was neglected. In a real observed protostar this effect would lead to an additional reddening in the left hand part of the HR diagram.

According to Fig. 6 to an outside observer the core of our protostar would look like an infrared point source of slowly increasing luminosity and effective temperature. Except for the rather short evolutionary phases at the beginning and at the end of the core's evolution, its "observable" parameters are in the range $30 \lesssim L/L_\odot \lesssim 3 \times 10^4$ and $100\,^\circ\text{K} \lesssim T_e \lesssim 400\,^\circ\text{K}$. These data are in

reasonable agreement with observed infrared sources and in particular with infrared sources of high luminosity like the source IRS 5 in W 3 (Wynn-Williams *et al.*, 1972). A comparison of the observed parameters of IRS 5 ($L \approx 3 \times 10^4\, L_\odot$, $T_e \approx 350\,°\mathrm{K}$) with Fig. 6 suggests that this infrared source is a massive protostar in the evolutionary phase where nuclear reactions have already started in the core, but which has not yet started to blow off its envelope. In this phase (which in our model calculations lasted $\sim 2.5 \times 10^4$ years) the core has still a rather low surface temperature and no ultraviolet radiation can penetrate into the thin outer layers to form an H II region, although the luminosity is already rather high. The present computations may therefore give a simple explanation for the absence of radio continuum radiation from IRS 5 and other luminous infrared point sources.

The numerical computations were carried out on the UNIVAC 1108 of the Gesellschaft für wissenschaftliche Datenverarbeitung Göttingen.

References

Appenzeller, I. 1970, *Astron. & Astrophys.* **5**, 355
Appenzeller, I. 1972, *Mitt. Astron. Ges.* **31**, 39
Auman, J. A., Bodenheimer, P. 1967, *Astrophys. J.* **149**, 641
Cox, A. N., Stewart, J. N. 1969, Academia Nauk, Scientific Information **15**, 1
Cox, J. P., Giuli, R. T. 1968, Principles of Stellar Structure, Gordon and Breach, New York, p. 335
Ecker, G., Kroll, W. 1965, JILA Report No. 37
Gaustad, J. E. 1963, *Astrophys. J.* **138**, 1050
Hayashi, C., Hoshi, R., Sugimoto, D. 1962, *Progr. Theor. Phys. Suppl.* No. 22
Hayashi, C. 1966, *Ann. Rev. Astron. & Astrophys.* **4**, 171
Hofmeister, E., Kippenhahn, R., Weigert, A. 1964, *Z. Astrophys.* **59**, 215
Krügel, E. 1971, Der Rosselandsche Mittelwert bei tiefen Temperaturen, Diplom-thesis, Göttingen 1971
Larson, R. B. 1969, *Monthly Notices Roy. Astron. Soc.* **145**, 271
Larson, R. B. 1972a, *Monthly Notices Roy. Astron. Soc.* **157**, 121
Larson, R. B. 1972b, Symposium on the Origin of the Solar System, Ed. H. Reeves, CNRS, Paris
Larson, R. B. 1973, *Ann. Rev. Astron. & Astrophys.* **11**, 219
Larson, R. B., Starrfield, S. 1971, *Astron. & Astrophys.* **13**, 190
Mihalas, D. 1967, *Methods in Computational Physics* **7**, 1
Narita, S., Nakano, T., Hayashi, C. 1970, *Progr. Theor. Phys.* **43**, 942
Pikel'ner, S. B. 1970, *Astrophys. Space Sci.* **7**, 489
Sahade, J. 1962, Symposium on Stellar Evolution, La Plata, p. 185
Vardya, M. S. 1960, *Astrophys. J. Suppl.* **4**, 281
Wynn-Williams, C. G., Becklin, E. E., Neugebauer, G. 1972, *Monthly Notices Roy. Astron. Soc.* **160**, 1

I. Appenzeller
W. Tscharnuter
Universitäts-Sternwarte
D-3400 Göttingen
Geismarlandstr. 11
Federal Republic of Germany